

AperTO - Archivio Istituzionale Open Access dell'Università di Torino

**Root morphology and biomechanical characteristics of high altitude alpine plant species and their potential application in soil stabilization**

**This is a pre print version of the following article:**

*Original Citation:*

*Availability:*

This version is available <http://hdl.handle.net/2318/1651676> since 2020-04-02T09:53:37Z

*Published version:*

DOI:10.1016/j.ecoleng.2017.05.048

*Terms of use:*

Open Access

Anyone can freely access the full text of works made available as "Open Access". Works made available under a Creative Commons license can be used according to the terms and conditions of said license. Use of all other works requires consent of the right holder (author or publisher) if not exempted from copyright protection by the applicable law.

(Article begins on next page)

1 **Root morphology and biomechanical characteristics of high altitude alpine**  
2 **plant species and their potential application in soil stabilization**

3  
4 **C. Hudek<sup>1,2\*</sup>, C. J. Sturrock<sup>3</sup>, B. S. Atkinson<sup>3</sup>, S. Stanchi<sup>1</sup>, M. Freppaz<sup>1</sup>**

5  
6 <sup>1</sup>University of Torino, DISAFA, Largo Paolo Braccini, 2, 10095 Grugliasco (TO), Italy

7 <sup>2</sup>T2M, Marie Curie Cofund Fellow

8 <sup>3</sup>Hounsfield Facility, School of Biosciences, The University of Nottingham, Sutton  
9 Bonington Campus, Nr Loughborough, LE12 5RD, UK

10 \*chudek@unito.it

11 **Abstract**

12  
13 Glacial forefields are young, poorly developed soils with highly unstable soil  
14 conditions. Root system contribution to soil stabilization is a well-known  
15 phenomenon. Identifying the functional traits and root morphology of pioneer  
16 vegetation that establish on forefields can lead us to useful information regarding the  
17 practical application of plants in land restoration of high altitude mountain sites.

18 This study aims to gather information on the root morphology and biomechanical  
19 characteristics of the 10 most dominant pioneer plant species of the forefield of Lys  
20 Glacier (NW Italian Alps).

21 X-ray Computed Tomography (X-ray CT) was used to visualize and quantify non-  
22 destructively the root architecture of the studied species. Samples were then cored  
23 directly from the forefield. Data on root traits such as total root length, rooting depth,  
24 root diameter, root length density and number of roots in relation to diameter classes

25 as well as plant height were determined and compared between species. Roots were  
26 also tested for their tensile strength resistance.

27 X-ray CT technology allowed us to visualize the 3D root architecture of species intact  
28 in their natural soil system. X-ray CT technology provided a visual representation of  
29 root–soil contact and information on the exact position, orientation and elongation of  
30 the root system in the soil core. Root architecture showed high variability among the  
31 studied species. For all species the majority of roots consisted of roots smaller than  
32 0.5 mm in diameter. There were also considerable differences found in root diameter  
33 and total root length although these were not statistically significant. However,  
34 significant differences were found in rooting depth, root length density, plant height  
35 and root tensile strength between species and life forms. In all cases root tensile  
36 strength decreased with increasing root diameter. The highest tensile strength was  
37 recorded for graminoids such as *Luzula spicata* (L.) DC. and *Poa laxa* Haenke and  
38 the lowest for *Epilobium fleischeri* Hochst.

39 The differences in root properties among the studied species highlight the diverse  
40 adaptive and survival strategies plants employ to establish on and thrive in the harsh  
41 and unstable soil conditions of a glacier forefield. The data determined and  
42 discovered in this study could provide a significant contribution to a database that  
43 allow those who are working in land restoration and preservation of high altitude  
44 mountain sites to employ native species in a more efficient, effective and informed  
45 manner.

46

47 Keywords: alpine species; glacier forefield; root phenotyping; soil stabilization; X-ray  
48 CT

49

50

51 **1. Introduction**

52

53 Glaciers in alpine regions are affected by climate change twice as much as the  
54 global average with respect to other ecosystems (Bradley et al., 2014) which  
55 results in accelerated glacial retreat. Retreating glaciers expose young soils that are  
56 low in nutrients (carbon and nitrogen) (Bradley et al., 2014; Lazzaro et al., 2010) and  
57 highly unstable (Matthews, 1999). Mass wasting and erosion processes are common  
58 in these forefields creating an inhospitable environment for plant colonization.  
59 Vegetation establishment on glacier forefields requires species with strong adaptive  
60 strategies and with high stress and disturbance tolerances (Robbins and Matthews,  
61 2009). In spite of the harsh environment, vegetation cover increases quickly  
62 (Matthews, 1999) due to the rapid colonization of pioneer species. Pioneer species  
63 can grow quickly on nitrogen poor soils due to their high reproduction capacity and  
64 photosynthetic activity, (Stöcklin and Bäumler, 1996) and tolerance against abiotic  
65 stresses e.g., extreme temperatures, ultraviolet radiation, atmospheric pressure,  
66 shortage of mineral nutrients (Jones and Henry, 2003 Körner, 2003; Stöcklin et al.,  
67 2009).

68 Successful colonization and establishment of alpine species on glacial forefields may  
69 provide important information on the practical aspects of land reclamation and  
70 habitat restoration (Robbins and Matthews, 2009). Root traits (architectural,  
71 morphological, physiological and biotic) play an important role in the physical and  
72 even though the present study will not discuss further, the chemical development of  
73 young soils (Bardgett et al., 2014; Massaccesi et al., 2015) bringing about increased  
74 structural stability in the forefield (Bardgett et al.,2014) and decreasing the frequency

75 and severity of any mass wasting and erosion processes. The biomechanical  
76 characteristics of roots such as tensile strength is a useful parameter for the  
77 quantification of the reinforcement potential; in particular for quantifying the added  
78 soil cohesion provided by plant roots. Determining the tensile strength of roots and  
79 their distribution in the soil profile can provide information on the increased shear  
80 strength of the soil provided by root reinforcement which can also determine plants'  
81 resilience to solifluction, frequently occurring in a periglacial environment (Jonasson  
82 and Callaghan, 1992). Quantitative data on root traits and architecture is one of the  
83 most significant variables considered when plants are evaluated for soil stabilization  
84 (Stokes et al., 2009). However data on root traits of alpine species remains scarce  
85 (Hu et al., 2013; Jonasson and Callaghan, 1992; Nagelmüller et al., 2016;  
86 Onipchenko 2014; Pohl et al., 2011; Zoller and Lenzin, 2006) which limits our  
87 understanding of the role these plants can play in root-soil interactions on the  
88 forefield.

89 Traditional techniques applied to examine the root system such as rhizotron or mini  
90 rhizotron, the use of paper pouches, synthetic soil media are all limited by the visual  
91 tracking of roots and/or creating an artificial environment that can lead to  
92 distorted/deceptive results. Destructive root phenotyping methods can also produce  
93 misleading results (Mooney et al., 2012) as they involve the separation of roots from  
94 the soil media meaning the relationship of the roots to the soil and to each other can  
95 no longer be observed (Pierrer et al., 2005). Additionally, repeated analysis on the  
96 same root system over time cannot be carried out e.g., dynamics of root growth or  
97 derivation of root demography (Koebernick et al., 2014).

98 Non-destructive imaging techniques such as Neutron Radiography, Magnetic  
99 Resonance Imaging (MRI) and X-ray Computed Tomography (X-ray CT) have been

100 effectively used in root phenotyping as they overcome the limitations of traditional  
101 techniques and able to provide results on intact root systems in undisturbed soil.  
102 Research involving modeling (e.g., Water Erosion Prediction Project (WEPP) or  
103 Chemicals, Runoff and Erosion from Agricultural Management Systems  
104 (CREAMS)) also benefits from the enhanced quality of numerical data on root traits  
105 provided by these state of the art techniques (Lobet et al., 2015; Tasser and  
106 Tappeiner, 2005).

107 X-ray CT has already been successfully employed in many studies focusing on plant  
108 roots (e.g., Aravena et al., 2011; Mooney et al., 2006; Pierret et al., 1999;  
109 Wantanabe et al., 1992) to obtain clear, 3D images of intact root systems in the soil  
110 without the paramagnetic (Materials that are attracted by an externally applied  
111 magnetic field and form internal, induced magnetic fields in the direction of the  
112 applied magnetic field. (Boundless, 2016)) impact on the image quality found in MRI  
113 (Mooney et al., 2012; Koebernick et al., 2014). Whilst the majority of X-ray CT  
114 studies have been carried out on agricultural species such as wheat (Jenneson et  
115 al., 1999; Gregory et al., 2003; Mooney et al., 2006), maize (Lontoc-Roy et al.,  
116 2006), soybean (Tollner et al., 1994), potato (Han et al., 2008) and tomato (Tracy et  
117 al., 2012), a few studies can be found on tree roots (Pierret et al., 1999; Kaestner et  
118 al., 2006; Paya et al., 2015) and grasses (Pfeifer et al., 2015). As yet, no research  
119 has been carried out on the root architecture of alpine species under natural soil  
120 conditions using the X-ray CT.

121 In the majority of these studies, sieved, pre-prepared low organic content soils were  
122 used as the plant growth matrix, as the greater amount of organic particles can make  
123 root differentiation from soil particles more difficult, hampering root segmentation  
124 (process of partitioning a [digital image](#) into multiple segments). Moreover, the

125 moisture distribution within undisturbed soil is more inconsistent which may also  
126 complicate the image segmentation process due to variations in image grayscale  
127 range of the roots under investigation (Pfeifer et al., 2015). While there have been a  
128 number of studies on the relationship between the natural soil matrix and the roots  
129 that permeate it, these studies have tended to focus on aspects of soil architecture  
130 rather than the architecture of the root (e.g., soil macropores, soil pore space) (e.g.,  
131 Hu et al., 2016; Kuka et al., 2013).

132

133 The aim of the present study is to investigate and compare the root architecture and  
134 root traits of the ten most dominant pioneer plant species of the forefield of Lys  
135 Glacier (NW Italian Alps) in their natural soil system by producing accurate 3D  
136 images of their root system using X-ray CT. The value of the X-ray CT is verified by  
137 comparing the obtained results with other commonly employed techniques.  
138 Moreover, root tensile strength measurements will be made to understand the  
139 biomechanical role of the plant species on soil stabilisation. The retrieved information  
140 is discussed in the light of the potential future use of the studied species for slope  
141 soil reinforcement.

142

143

## 144 **2. Materials and methods**

145

### 146 **2.1 Study site**

147

148 Plant sampling was carried out on the recently deglaciated forefield of the Lys  
149 Glacier in the Aosta Valley (North West Italy). The glacial till was deposited in 2004

150 at an altitude of 2300 m above sea level on a bedrock of granitic gneiss and  
151 paragneiss belonging to the Monte Rosa nappe (D'Amico et al., 2014). The climate  
152 is alpine subatlantic with a mean annual rainfall of 1200 mm. The mean annual air  
153 temperature is -1 °C (Mercalli, 2003) with a winter temperature below -4 °C on  
154 average. The sampling site is south facing with a soil texture of loamy sand and an  
155 udic moisture regime (Soil Survey Staff, 2010). The chemical properties of the soil at  
156 the study site correspond to a slightly acidic soil (pH 5.8 - 6.7) with very low amounts  
157 of total nitrogen (TN) and total organic carbon (TOC) (0.002-0.017 g kg<sup>-1</sup> and 0.018-  
158 0.217 g kg<sup>-1</sup> respectively) with available phosphorus (P) of 1.3-4.7 mg g<sup>-1</sup>. Pioneer  
159 alpine plants, mostly graminoid and forb species colonize the site (e.g., *Epilobium*  
160 *fleischeri* Hochst., *Linaria alpina* (L.) Mill., *Trisetum distichophyllum* (Vill.) P.  
161 Beauve.), a detailed vegetation survey of the moraine can be found in D'Amico et al.  
162 (2014).

163

## 164 2.2 Sampling approach

165

166 The ten most common plant species of the forefield were selected. These were  
167 sampled between August and September 2015; *E. fleischeri*, *T. distichophyllum*,  
168 *Trifolium pallescens* Schreb., *Luzula spicata* (L.) DC., *Silene exscapa* All., *Minuartia*  
169 *recurva* (All.) Schinz and Thell., *Festuca halleri* All. *Poa laxa* Haenke, *Salix helvetica*  
170 Vill. and *Leucanthemopsis alpina* (L.) Heyw (Table1). A total of 60 soil columns, (i.e.  
171 6 columns per species) were excavated. During sampling, special care was taken to  
172 avoid individuals with any visible neighbouring plant effects (Gaudet and Keddy,  
173 1988) and to keep plant size as equal as possible for all 60 samples. One sample  
174 from each species was cored 10 samples in total) with their own PVC cylinder



175 (maximum sample height of 20 cm x diameter of 7.4 cm). After coring, the ten soil  
 176 columns were carefully secured and placed in plastic bags and transported to the  
 177 laboratory. In the laboratory the cored samples were placed in a climate chamber  
 178 until the X-ray CT tests were undertaken. The climate chamber was set to provide  
 179 conditions so as to delay root decay using a photoperiod of 14 hours, a relative  
 180 humidity of 65 % and temperatures of 15 °C by day and 10 °C by night.  
 181 The remaining five replicates of each species (a total of 50) were excavated with a  
 182 trowel. The 50 soil columns containing the root system of the individuals were placed  
 183 in plastic bags, transported to the laboratory and stored at 3.5 °C until  
 184 measurements were undertaken (Bast et al., 2015).  
 185 Table1.

Species	Common name	Life form	Succession	Family
<i>Epilobium fleischeri</i> Hochst.	Alpine willowherb	Forb	Early	Omagraceae
<i>Trisetum distichophyllum</i> (Vill.) P.Beauve.	Tufted hairgrass	Graminoid	Early	Poaceae
<i>Trifolium pallescens</i> Schreb.	Pale clover	Forb	Early	Fabaceae
<i>Luzula spicata</i> (L.) DC.	Spiked woodrush	Graminoid	Mid	Juncaceae
<i>Silene exscapa</i> All.	Moss campion	Forb	Mid	Caryophyllaceae
<i>Minuartia recurva</i> (All.) Schinz and Thell.	Recurved sandwort	Forb	Late	Caryophyllaceae
<i>Festuca halleri</i> All.	Haller's Fescue	Graminoid	Late	Poaceae
<i>Poa laxa</i> Haenke	Banff Bluegrass	Graminoid	Ubiquitous	Poaceae
<i>Salix helvetica</i> Vill.	Swiss willow	Dwarf shrub	Ubiquitous	Salicaceae
<i>Leucanthemopsis alpina</i> (L.) Heyw.	Alpine Moon Daisy	Forb	Ubiquitous	Asteraceae

186

### 187 2.3 Non-destructive root phenotyping

188

189 The cored samples from the PVC cylinder were scanned using a Phoenix V|TOME|X  
 190 M 240 high resolution X-ray CT system (GE Sensing and Inspection Technologies,  
 191 Wunstorf, Germany). The scanning parameters (Table 2) were optimized to allow  
 192 balance between a large field of view and a high resolution. Due to the height of the  
 193 cylinder (20 cm) two separate scans (upper and lower part of the sample) were

194 made to cover and image the entire sample. Each sub-scan was then reconstructed  
195 using DatosRec software (GE Sensing and Inspection Technologies, Wunstorf,  
196 Germany) and then manually combined in VG Studio MAX v2.2 (Volume Graphics  
197 GmbH, Heidelberg, Germany) and exported as a single 3D volumetric dataset. To  
198 distinguish the root system from the soil material image processing techniques were  
199 applied. Roots were segmented from the reconstructed CT data by using the region  
200 growing method (Gregory et al., 2003) in VG Studio MAX v2.2. Quantification of 3D  
201 root traits was undertaken using RooTrak software (Mairhofer et al., 2012). RooTrak  
202 was able to provide quantitative data on the root volume (total mass of the root  
203 system; mm<sup>3</sup>), root area (root area in direct contact with the soil; mm<sup>2</sup>), the root  
204 system's maximum vertical and horizontal length (mm) as well as the convex hull  
205 (the region of soil explored by the root system; mm<sup>3</sup>) (Mairhofer et al., 2015).

206

207 **Table 1** Scanning parameters for X-ray CT.

208

209 2.4 Destructive root phenotyping

210

211 Following X-ray CT scanning, the roots were extracted from the soil column by  
212 carefully cleaning the soil matrix from the roots with a water jet under a sieve mesh  
213 to retain remnants of roots that may come loose during the cleaning process. The  
214 washed roots were then placed into a 15 % ethanol solution and stored at 3.5 °C.  
215 Then the root systems were scanned with a flatbed scanner (EPSON Expression  
216 11000XL). The images from scanning had a 600 dpi resolution and were used for  
217 two dimensional image analysis. This was with the aim to compare the CT scanned  
218 results with the results of a, traditional technique (Paez-Garcia et al., 2015). Root

219 traits such as total root length, average root diameter, and the root system's  
220 maximum vertical and horizontal length were considered for analysis.

221 The remaining 50 plant samples (five replicates of each species were followed the  
222 same cleaning, storing and scanning method as before . All 2D scanned images  
223 were analyzed with the WinRHIZO 2013e and ImageJ software. The data collected  
224 on root traits were total root length, root length distribution (%) in different diameter  
225 classes, average root diameter, root length density, rooting depth and total plant  
226 height. Additionally plant height was measured according to the standardized  
227 measurement of plant functional traits (Pérez-Harguindeguy et al., 2013).

228

## 229 2.5 Root tensile strength

230

231 Root tensile strength tests were performed to determine root resistance to breaking  
232 under tension ([Bischetti et al., 2005](#); Pohl et al., 2011). The complete root system,  
233 kept in a 15 % ethanol solution was first cut into individual root segments. Randomly  
234 selected undamaged roots with the widest available range of diameters were then  
235 selected for testing. Before testing, root diameter at three points of the root segment  
236 were measured with a digital caliper to obtain the average root diameter of the  
237 individual root sample. This is necessary as the exact position of root rupture is  
238 unknown before testing.

239 Root tensile strength were measured in the laboratory using an electromechanical  
240 universal testing machine, MTS Criterion, Model 43 (MTS Systems, Eden Prairie,  
241 MN, USA). Plant roots were secured between clamps at both ends. The clamps  
242 consist of two metal discs (washers) covered with drafting tape holding the roots in  
243 place. The speed reduction of the device was maintained at a steady 10 mm min<sup>-1</sup> as

244 it was suggested in other studies (Bischetti et al., 2005; Bordoni et al., 2016; De  
245 Baets et al., 2008; Yang et al., 2016) and the tensile force was measured by a load  
246 cell (500N) connected to a computer to record the results. Roots broke when they  
247 could no longer resist tensile force. Measurement results were excluded from data  
248 analysis when root rupture occurred near the clamp. Measurement considered to be  
249 successful when the rupture occurred in the middle of the root section

250

## 251 2.6 Statistical analysis

252

253 In the present study comparative data analysis on root traits between the non-  
254 destructive and destructive technique was only respected when comparing the  
255 maximum vertical and horizontal length of the root system due to the lack of data  
256 available on very fine roots ( $< 0.5$  mm) on the 3D images.

257 Results obtained from X-ray CT scanning (RooTrak) on the root system's maximum  
258 vertical and the maximum horizontal length were compared with results obtained  
259 from the destructive method (ImageJ) by applying Pearson's correlation test. Once  
260 the normality and homogeneity of variance were verified a one-way analysis of  
261 variance (ANOVA) was used to detect differences in the measured root properties  
262 (root length density, total root length, mean root diameter, rooting depth, root length  
263 distribution within diameter classes) and plant height among the studied species. In  
264 cases when significant differences were found between the groups, the Tukey post  
265 hoc test was run to detect where the differences occurred between the groups.

266 The relationship between root tensile strength and root diameter was evaluated by  
267 fitting a regression curve (power law equation). Analysis of covariance (ANCOVA)  
268 was performed to compare tensile strength results between the 10 studied species

269 and to take root diameter into consideration as a covariant. Both tensile strength and  
270 root diameter values were log transformed before the analysis. All assumptions were  
271 tested before carrying out ANCOVA (linearity, homogeneity and normality) . All  
272 statistical analysis was carried out using the statistical software SPSS Statistics 22  
273 (IBM SPSS, 2013).

274

### 275 **3. Results**

276

#### 277 **3.1 Non-destructive root phenotyping**

278

279 X-ray CT was successfully used to reveal the 3D root architecture of the studied 10  
280 species. Tap roots and thicker lateral roots (diameter >0.5 mm) were identified in all  
281 cases while individual examples of thinner lateral roots (diameter < 0.5 mm) were  
282 only identified for *S. helvetica*, *P. laxa*, *L. spicata* and *F. halleri*, (diameters of 0.35,  
283 0.35, 0.25 and 0.25 mm, respectively). Even though it was not possible to extract the  
284 entire root system, a visual representation of root–soil contact in the undisturbed  
285 position, orientation and elongation of the core root system was possible. It should  
286 be noted that due to the size limitation of the PVC cylinder and the difficulty of  
287 identifying root position when coring, the tap root and/or lateral roots were cut off by  
288 the edge of the cylinder therefore the max vertical and horizontal root length in the  
289 present study is approximate and should only be taken into consideration as part of  
290 data validation for RooTrak.

291

292 The maximum vertical and horizontal root length data obtained from the 3D images  
293 were underestimated by an average of 42% and overestimated by 26% respectively

294 when compared to measured data with ImageJ. The results from the Pearson's  
295 correlation tests between RooTrak and ImageJ showed a weak positive correlation  
296 ( $r= 0.57$ ,  $p=0.084$ ) for maximum vertical root length (Figure 3a) and a very weak  
297 negative correlation ( $r= -0.38$ ,  $p=0.275$ ) for the maximum horizontal root length  
298 (Figure 3b). Because the p-values are greater than the significance level of 0.05,  
299 there is inconclusive evidence about the significance of the association between the  
300 variables.

301

302

303

304 The highest root volume, root area and convex hull (Table 3) were all recorded for *T.*  
305 *pallescens* (1530 mm<sup>3</sup>, 7752 mm<sup>2</sup>, 505384 mm<sup>3</sup> respectively). The lowest root  
306 volume was recorded for *M. recurva* and *P. laxa* (144 and 150 mm<sup>3</sup> respectively)  
307 while the lowest value of root area (1146, 1547 and 1677 mm<sup>2</sup>) and convex hull  
308 (24117, 45612, 60237 mm<sup>3</sup>) was recorded for *S. helvetica*, *P. laxa* and *M. recurva*  
309 respectively. Results from *F. halleri* and *L. spicata* were excluded from the  
310 comparison as it was difficult to identify and segment the high number of fine (< 0.25  
311 mm), overlapping roots and in many cases it was not possible at all. Therefore  
312 including the results of *F. halleri* and *L. spicata* would have caused misleading  
313 overall results.

314

315

316

317 **Table 3.** Values of root traits analyzed with RooTrak (volume, area, maximum  
318 vertical and horizontal length of the root system, convex hull), ImageJ (maximum

319 vertical and horizontal length of the root system) and WinRHIZO (total root length  
320 and average root diameter) of the X-ray CT scanned samples.

321

322 The highest total root length was recorded for *T. distichophyllum*, *L. spicata* and *S.*  
323 *exscapa* (192.7, 100.3 and 95.3 m respectively) and the lowest for *P. laxa* and *F.*  
324 *halleri* (10.5 and 20.7 m respectively). The rest of the species results fell between the  
325 values of 50.5 and 62.2 m (Table 3).

326

327 Average root diameter ranged between 0.16 and 0.31 mm. The lowest root  
328 diameters were recorded for *L. spicata* and *E. fleischeri* (0.16 mm and 0.17 mm  
329 respectively) and the highest for *P. laxa* and *T. pallescens* (0.31 mm and 0.30 mm  
330 respectively) (Table 3).

331

332 **Figure 3** a., Linear correlation between RooTrak and ImageJ data on the maximum  
333 vertical and b., horizontal root length for the 10 studied alpine species.

334 The overall root architecture for each species displayed considerable variation  
335 (Figure 1 a-j). To determine and differentiate root system architecture between the  
336 species the root type classification established by Lichtenegger and Kutschera,  
337 (1991) was applied:

338 *E. fleischeri* showed a dominant pole root system with strong horizontal root  
339 spreading indicating the intense clonal growth of the plant. *T. pallescens* showed a  
340 cone shape and *S. exscapa* a wider cone shape upward extended root type. *S.*  
341 *helvetica* and *M. recurva* had a discoid shaped root system due to the shallow depth  
342 of rooting but large lateral spreading. *P. laxa*, *F. halleri* and *L. spicata* all showed a

343 cone shape downwards dilated root type while *L. alpine* had an umbrella shaped and  
344 *T. distichophyllum* a cylindrical shaped root type.

345

346 **Figure1.** Root architecture of the 10 studied pioneer alpine species detected by X-  
347 ray CT scanning. Scale bars: a., 35 mm, b., 25 mm, c., 40 mm, d., 15 mm, e., 10  
348 mm, f., 15 mm, g., 15 mm, h., 30 mm, i., 45 mm, j., 20 mm.

349

350 **Figure 2** a., Image of the core root system b., the core root system in relation to the  
351 soil matrix and c., the washed entire root system of *T. pallescens*. Scale bar a.,  
352 45 mm b., 40 mm and c., the ruler uses cm.

353

354 The natural soil matrix showed a great variation in terms of soil structure among the  
355 cored samples. Figure 5 a-c shows examples of the structural diversity of the  
356 samples. The soil matrix in Figure 5 a., indicates a deposition of glacial till with little  
357 reorganization due to slope processes as Figure 5 b., and c., are fluvio-glacial and  
358 lake depositions with visible silt and sand layers.

359

360 **Figure 5** Examples of the grayscale CT images of the soil matrices a., glacial till with  
361 *T. distichophyllum* b., and c., fluvio-glacial and lake depositions.

362

### 363 3.2 Destructive root phenotyping

364

365 Root length density results varied greatly among the studied species (9.3–85 cm cm<sup>-3</sup>  
366 <sup>3</sup>). The lowest density was recorded for *E. fleisheri*, *M. recurva* and *T. pallescens*,  
367 with 9.3, 29 and 33 cm cm<sup>-3</sup> respectively and the highest was recorded for *T.*



368 *distichophyllum* and *L. spicata* with 85 and 81 cm cm<sup>-3</sup> respectively. There was  
369 significant difference found in root length density among the species (F (9, 22) =  
370 4.78, p <0.001). Post-hoc comparisons using the Tukey HSD test indicated that root  
371 length density differed significantly (p <0.05) between *E. fleischeri* and *L. spicata*, *T.*  
372 *distichophyllum*, *S. helvetica* and *F. halleri* as well as between *M. recurva* and *L.*  
373 *spicata*. There was no statistically significant difference in root length density  
374 between the other species. However, the difference between *T. pallescens* and *L.*  
375 *spicata* showed a substantial trend toward significance (p=0.078) as well as between  
376 *M. recurva* and *T. distichophyllum* (p=0.062). Specifically, the results suggest that  
377 out of the ten studied species, only *E. fleischeri*'s and *M. recurva*'s root system  
378 resulted in a significantly lower root length density when compared to the majority of  
379 the studied plants. It should be noted that in most but not all cases, higher root  
380 length density was found among the graminoid (*L. spicata*, *T. distichophyllum*, *F.*  
381 *halleri*) and the dwarf shrub (*S. helvetica*) species.

382

383 Total root length results (Table 4) showed no significant differences between the  
384 species (F (9, 39) =1.07, p=0.417) even though the mean results showed moderate  
385 variability among them (75.3–368.5 m). The shortest length was recorded for *E.*  
386 *fleischeri*, and *S. exscapa*, with 75.3 and 106.2 m respectively and the highest for *L.*  
387 *alpina* and *S. helvetica* with 368.5 and 342.3 m respectively.

388

389 **Table 4** Plant height (mm), rooting depth (mm) measured with ImageJ, total root  
390 length (m), mean root diameter (mm) and root length density (cm cm<sup>-3</sup>) of the 10  
391 studied alpine species measured with WinRhizo.

392

393 Table 5 shows the root length distribution in different diameter classes (%). Eight out  
394 of ten species had their highest root count (57-36 %) in the diameter class  $0 < L \leq 0.1$   
395 mm with the exception of *T. distichophyllum* and *S. helvetica* which had it at  
396  $0.1 < L \leq 0.2$  (41 %) and  $0.2 < L \leq 0.3$  mm (37 %) respectively. *T. pallescens* and *S.*  
397 *helvetica* also had roots larger than 2 mm in diameter as the other species rarely  
398 exceeded 1 mm in diameter.

399

400 **Table 5** Root length distribution (%) of the 10 pioneer alpine plants in relation to  
401 different diameter classes (mm).

402 Figure

403

404 The mean root diameter results (Table 3) also showed no significant differences  
405 between the species ( $F(9, 22) = 1.78, p = 0.129$ ) values. The results ranged between  
406 0.21 mm and 0.47 mm. The lowest mean root diameter was recorded for *T.*  
407 *distichophyllum* with 0.21 mm and the highest for *T. pallescens* with 0.47 mm.

408

409 Rooting depth results (Figure 6), determined by ImageJ showed considerable  
410 variation among the species, ranging from 9 to 19.7 cm. The deepest penetrating  
411 root system was recorded for *E. fleischeri* and the shallowest for *S. helvetica*. A one-  
412 way ANOVA was used to compare the rooting depth results between the 10 species  
413 which showed significant difference at  $F(9, 38) = 2.38, p < 0.03$ . The Tukey HSD test  
414 indicated that *E. fleischeri* had a significantly ( $p < 0.05$ ) longer rooting depth than *S.*  
415 *helvetica* and *F. halleri*.

416 Plant height also varied between the species, ranging from 15 to 65 cm. The highest  
417 plant height was recorded for *E. fleischeri* and the lowest for *M. recurva*. There was

418 significant differences found at  $F(9, 29) = 57.73$ ,  $P < 0.000$  between the studied  
419 species.

420

421 **Figure 6** Plant height (cm) and rooting depth (cm) of the 10 studied alpine plant  
422 species.

423

424

### 425 3.3 Root tensile strength

426

427 There was a great variation in the tensile strength results among the studied species  
428 (Table 5). The highest mean tensile strength was found at the graminoid and shrub  
429 species ranging between 138-86 MPa and the lowest among the forbs ranging  
430 between 60-29 MPa. The results showed that graminoid species have comparable  
431 tensile strength results to the dwarf shrub *S. helvetica*. When the significant  
432 differences were tested between the studied species taken root diameter into  
433 consideration as a covariate the results showed significant differences between the  
434 studied species at  $F()=$ ,  $p < 0$ .

435 Tensile strength and the related root diameter values were plotted (Figure 7) to show  
436 the relationship between root tensile strength and root diameter which confirmed the  
437 power law relationship meaning that with increasing root diameter root tensile  
438 strength decreased.

439

440 **Table 6** Life forms, the number of samples (n) tested, the range of root diameters  
441 (mm), root tensile strength (MPa) values, scale factor ( $\alpha$ ) rate of strength decrease  
442 ( $\beta$ ) and the goodness of fit ( $R^2$ ) of the 10 studied alpine species.

443

444 **Table 7** ANOVA table with multiple comparisons of root tensile strength (MPa)  
445 between the studied plant species.

446

447 **Figure 7** The relationship between root tensile strength (MPa) and root diameter  
448 (mm) for the 10 studied alpine species

449

450

## 451 **4. Discussion**

452

### 453 4.1 Non-destructive root phenotyping

454

455 The X-ray CT scanning has provided the first ever 3D images of the intact core root  
456 system of 10 different pioneer alpine plant species in their natural soil matrix. Visual  
457 information on the vertical and horizontal spreading as well as the rooting angle and  
458 branching of thicker roots in connection to the soil matrix were visible and could be  
459 important information when determining the significance of the root system on soil  
460 reinforcement in future studies (e.g. the resistance of the root system to uprooting or  
461 its protective role against shallow landsliding). During the use of X-ray CT several  
462 challenges and limitations were discovered; The following aspects made it difficult to  
463 decide on the scanning parameters: There was a limited amount (Stöckli and  
464 Bäumler, 1996; Pohl et al., 2011) or no data available on the root traits of the studied  
465 species prior to testing. They also had varying characteristics in terms of life form,  
466 family (Körner, 2003; Pignatti, 2003; Broglio and Poggio, 2008) and succession  
467 (Damico et al., 2014; Stöcklin and Bäumler, 1996) indicating different root

468 architecture and anatomy. Additionally they had never been subject to study with  
469 current state of the art phenotyping techniques. The samples were cored from their  
470 natural habitat in a heterogenic soil matrix and the soil absorbed a high level of the  
471 X-rays resulting in prohibitively long scans to achieve the necessary beam  
472 penetration. The tracking of individual roots during segmentation was extremely  
473 difficult as the heterogenic soil matrix made it difficult to differentiate roots from other  
474 organic particles in the soil (Figure 4 a, b, and c). Additionally the root system  
475 contained vast amounts of overlapping roots and neighbouring plant roots were  
476 invariably cored together with the test sample even when, from the surface, samples  
477 appeared free from any neighbouring plant effects.

478 Roots with a diameter  $>0.5$  mm are visible on the 3D images, these thicker roots  
479 allow us to estimate the location of thinner roots (Stokes et al., 2009). Not being able  
480 to detect the thinner roots on the present 3D images was not due to the limitations of  
481 the X-ray CT technology, rather the issue of resolution, sample size and the  
482 heterogenic soil matrix. In general, in homogeneous background the minimum  
483 resolution should be set twice as high as the cored sample is long in millimeters and  
484 set even higher if the background is heterogenic (Kaestner et al., 2006). A higher  
485 resolution setting however would have resulted in a prohibitively prolonged scanning  
486 and segmenting time. The method suggested by Kaestner et al. (2006) was  
487 successful at detecting roots with a diameter  $<0.5$  mm in homogeneous background  
488 however roots in heterogeneous soil matrix (Figure 4 a-c) remained challenging.  
489 Cored samples of reduced length and diameter may have allowed for the detection  
490 and segmentation of the finer roots within the system but the compromise would be  
491 the smaller PVC cylinders would not have been suitable for sampling the species  
492 from the field without causing damage i.e. preventing disturbed soil conditions within

493 the sample. A factor to possibly bear in mind for future work conducted on alpine  
494 species with fine root systems would be to take two sets of cores when assessing  
495 the different scales in root architecture.

496 Interestingly, although it was not possible to segment using the available software;  
497 many of the fine roots were often visible to the naked eye when manually scrolling  
498 through the greyscale images providing a unique insight into the complexity of these  
499 alpine species.

500

501

502

#### 503 4.2. Analysis of root architecture and root traits

504 *S. exscapa* and *T. pallescens* both have a dominant tap root morphology with a large  
505 number of tillers. Their tap root and thicker lateral roots are often found growing  
506 through cracks in the bedrock thereby anchoring the plant and stabilizing the soil  
507 from shallow landsliding. The number of lateral roots and the diversity of their  
508 branching angles resulting in a larger shear zone indicate an increased soil stability  
509 (Abe and Ziemer, 1991). Both *S. exscapa* and *T. pallescens* have dense, fine root  
510 networks that can play an important role in reducing soil erosion. Root nodules are  
511 clearly visible on the roots of *T. pallescens* reflecting the existing association the  
512 plant has with symbiotic nitrogen-fixing bacteria (Holzmann and Haselwandter,  
513 1988).

514 *S. helvetica* also has a dominant taproot morphology with the potential of growing  
515 through cracks in the bedrock though it has a shallower rooting depth than *S.*  
516 *exscapa* or *T. pallescens*. *S. helvetica* has a large lateral spread in the upper soil

517 layer with a dense fine root network which can provide increased support in soil  
518 erosion control and horizontal anchoring.

519 Due to the uniform length of the umbrella shaped root system of *L. alpina* it can be  
520 easily uprooted (cit), therefore, its potential as soil reinforcement is greatly limited  
521 although it is capable of trapping a significant amount of soil due to its dense fine  
522 root network (Hudek et al., 2017) and reducing soil erosion.

523 The dominant pole type of root system of *E. fleischeri* showed the greatest rooting  
524 depth with intensive rhizome spreading. The main feature of the plant's strategy is  
525 rapid colonization of open space through wide lateral clonal spreading (Stöckli and  
526 Bäumler, 1996) which is a typical strategy for early successional plants such as  
527 *Hieracium staticifolium* All., *Achillea moschata* (Wulfen) or *Cerastium pedunculatum*  
528 Gaudin (Stöckli and Bäumler, 1996). Its root system does not have notable  
529 anchoring properties, its survival strategy relies on an elaborate network of rhizome  
530 spreading, widely spaced ramets and rapid colonization (Alpandino, 2011). In this  
531 way the plant is able to quickly overcome diverse mass wasting processes.  
532 Additionally its short and fragile fine root (<1mm) network is unclearly able to provide  
533 additional soil stabilization (Bischetti et al., 2009) even though plant biomass and  
534 allometry are stated being a significant element when plants are evaluated for soil-  
535 root reinforcement (Gonzalez-Ollauri and Mickovski, 2016). In general the function of  
536 these roots is limited to water and nutrient uptake to support plant growth (Stokes et  
537 al., 2009; Tasser and Tappeiner, 2005).

538 *T. distichofillum* also uses horizontal spreading through clonal growth as a strategy  
539 for rapid colonization but with shorter distance between ramets (Alpandino, 2011). It  
540 also has a dense lateral root system with moderate rooting depth and a high  
541 percentage of fine and very fine roots throughout the entire root system. This can

542 make the plant more resilient to uprooting and at the same time, through the  
543 elaborate network of rhizome spreading, able to overcome diverse mass wasting  
544 processes (Körner, 2003). Its dense fine and very fine roots trap soil providing  
545 erosion control. *P. laxa* is a plant with clumped clonal growth form with short distance  
546 between ramets. *F. halleri* and *L. spicata* both form compact tussocks with a dense  
547 fibrous root system. This phalanx type of clonal growth results in a slow horizontal  
548 spreading (Alpandino, 2011). These types of root morphology can make the plants  
549 extremely resilient to uprooting and a potentially effective plant in erosion control.

550 The root architecture of the species showed a wide range of root types dictated by  
551 genetic characteristics (Gray and Sotir, 1996) and environmental factors e.g.,  
552 nutrient availability or soil temperature (Nagelmüller et al., 2016; Khan et al., 2016).  
553 Root plasticity too has effects on root architecture, it is essential in coping with and  
554 overcoming stress (Bardgett et al., 2014; Poorter et al., 2012; Stöcklin and Bäumler,  
555 1996) as well as strengthening the resilience of pioneer species to the harsh  
556 environmental conditions.

557 Even though *E. fleischeri* had a significantly higher rooting depth compared to the  
558 other species, in general, rooting depth was uniformly shallow which is in line with  
559 previous findings (Lichtenegger, 1996; Jonasson and Callaghan, 1992; Pohl et al.,  
560 2011) on alpine species. This is influenced by two main controlling environmental  
561 factors; soil temperature and water availability (Lichtenegger, 1996; Körner, 2003).  
562 Alpine vegetation in general have a shallower rooting system than species from  
563 lowlands as at high altitudes with increasing soil depth, soil temperature and water  
564 fluctuations decrease at a higher rate than in the lowlands (Lichtenegger, 1996). This  
565 also can reflect on root distribution within the different soil horizons, indicating that



566 the high root density in the upper soil layer quickly decreases with increasing soil  
567 depth (Lichtenegger, 1996).

568 Root length density has a great influence on soil stability (Bardgett et al., 2014;  
569 Stokes et al., 2009) by altering the hydrological properties of the soil and increasing  
570 the resistance of the roots for disruptive forces. All studied species had a large  
571 amount of fine and very fine roots which is common in alpine species (Körner, 2003;  
572 Pohl et al., 2011). In general, fine and very fine roots have a rapid turnover supplying  
573 a large amount of carbon to the soil and increasing the organic content of the soil.  
574 Together with the physical and chemical contribution they gradually increase the  
575 aggregate stability of the soil which reduces the susceptibility of the soil to erosion  
576 processes (Pohl et al., 2011; Hudek et al., 2017). Additionally, both live and dead  
577 roots provide potential preferential flow paths in hillslopes, securing the stability of  
578 the soil by reducing pore water pressure (Ghestem et al., 2011). On the other hand,  
579 bypass flow can lead to perched water tables, saturating the soil that can develop  
580 positive pore-water pressure that could trigger landslides (Ghestem et al., 2011).  
581 Glacier forefields are nutrient limited soils; fine and very fine roots (< 0.5 mm)  
582 however, provide strong symbiotic links between the plant and the fungus systems  
583 and it has been proven that mycorrhizal fungi increases the water and nutrient  
584 uptake of the plant (Smith and Read, 2008) and promotes root growth (Ola et al.,  
585 2015) which also influences RLD (Bast et al., 2014; Graf and Frei 2013; Tisdall,  
586 1991). The dense fine root system of the studied species is also able to mechanically  
587 bind the soil particles thereby contributing to increased soil stabilization (Pohl et al.,  
588 2011; Norris et al., 2008).

589 In the present study the total root length values showed non-significant difference  
590 between the species and life forms while the highest values were recorded among

591 the graminoid species as was with the work of Pohl et al. (2011) though in the  
592 present study the measured values greatly exceed those of Pohl et al. (2011). This  
593 can be attributed to the fact that at the sampling site of Pohl et al., (2011) sampling  
594 was carried out on managed ski slopes where soil compaction inhibits root growth  
595 (Nagel et al., 2012; Pfeifer et al., 2014) while in the case of our study on the recently  
596 deglaciaded forefield, sampling was performed on a site relatively free from human  
597 interference and soil compaction was not an inhibiting factor for root growth.

598 Under natural conditions species grow together creating a complex underground root  
599 network/structure due to the diversity of root types, enlarging the protective role of  
600 plants on soil stabilization at different levels and soil layers (Pohl et al., 2009;  
601 Reubens et al., 2007). Plant richness should therefore be encouraged when plants  
602 are considered for soil conservation purposes such as land reclamation.

603

#### 604 4.3. Root tensile strength

605

606 The tensile strength results of the present study were 3-7 times higher than those  
607 found in literature data on the same alpine species (*L. spicata*, *L. alpina*) (Pohl et al.,  
608 2011) and other alpine and arctic graminoid and forb species (Pohl et al., 2011,  
609 Jonasson and Callaghan, 1992). Root tensile strength is mainly effected by the  
610 genetic properties of the plant (Gray and Sotir, 1996) while additional factors such as  
611 age (Reubens et al, 2007), ecological conditions and management  
612 practices(Bischetti et al., 2009) can result in varying tensile strength values for the  
613 same species. Gonzalez-Ollauri et al. (2017) highlighted that root tensile strength  
614 can vary with changes in root moisture content which closely links to soil moisture  
615 content (i.e. dry roots have a lower level of tensile strength compare to roots with

616 optimum root moisture). Root diameter has direct influence on root tensile strength  
617 as root tensile strength is calculated by the ratio between the breaking force (N) and  
618 the root cross section area ( $\text{mm}^2$ ) which depends on root diameter (Bischetti et al.,  
619 2016). In general, fine and medium size roots (in diameter 0.01-10.00 mm) have  
620 higher values of tensile strength compared to roots with a larger diameter ( $> 10.00$   
621 mm). Larger sized roots act primarily as individual anchors mobilising only a small  
622 amount of their tensile strength before slipping through the soil (Bischetti et al.,  
623 2005). However, fine and medium sized roots can mobilize their entire tensile  
624 strength and due to their higher surface area, have superior resistance to uprooting  
625 (Gray and Sotir, 1996). In the present study the diameter of the tested roots ranged  
626 between 0.03 mm and 1.66 mm, these values are smaller than what is found in the  
627 literature data which can be one of the explanation for the considerably higher tensile  
628 strength results. Additionally the samples in Pohl et al. (2011) were collected from a  
629 managed ski slope which confirms results observed by Bischett et al. (2009) that  
630 ecological conditions and management can alter tensile strength.

631 It was possible to demonstrate the significant relationship between tensile strength  
632 and root diameter the plotted tensile strength results can demonstrate the power law  
633 relationship and can be used to make comparisons between species.

634

## 635 **5. Conclusions**

636

637 This study aimed to provide information on root morphology and root traits on  
638 pioneer alpine species from a recently deglaciated site in the Italian Alps with the  
639 view to determine the plants' efficiency in soil stabilization. To provide unique visual  
640 3D data on the root architecture of a wide variety of alpine pioneer species under

641 intact natural soil conditions, we applied a state of the art non-destructive plant  
642 phenotyping technique, X-ray CT. This is the first study that uses the X-ray CT  
643 technique to image the root system of alpine plants undisturbed in their natural  
644 alpine soil matrix.

645 Results showed great variation in global root architecture between the studied  
646 species. X-ray CT could successfully identify roots >0.25, 0.35 mm in diameter at the  
647 resolution used for scanning. With complementary use of destructive phenotyping  
648 techniques, quantitative data on root traits and the plants biomechanical  
649 characteristic allowed us to determine species' efficiency in soil stabilization. The  
650 high tensile strength results of graminoid and the dwarf shrub species combined with  
651 a dense elaborate root morphology, provide many anchoring points and enhanced  
652 plant resilience to solifluction in a periglacial environment. While forbs longer,  
653 anchoring root system with lower but comparable tensile strength to the garminoid  
654 and dwarf shrub species, could advocate their suitability as protection against  
655 shallow landsliding. With the exception of one or two species (*E. fleischeri*, *M.*  
656 *recurva*) all studied plants play an important role in soil erosion control due to their  
657 dense elaborate fine and very fine root system.

658

659

## 660 **Acknowledgements**

661 This research was enabled by the Transnational Access capacities of the European  
662 Plant Phenotyping Network (EPPN, grant agreement no. 284443) funded by the FP7  
663 Research Infrastructures Programme of the European Union. As well as receiving  
664 funding from the European Union's Horizon 2020 research and innovation  
665 programme under the Marie Skłodowska-Curie grant agreement No 609402 - 2020

666 researchers: Train to Move (T2M). The Hounsfield Facility received funding from  
667 European Research Council (Futureroots Project), Biotechnology and Biological  
668 Sciences Research Council of the United Kingdom and The Wolfson Foundation.  
669 The authors wish to thank Alessio Cislighi, Enricho Chiaradia and Gian Battista  
670 Bischetti for the access to and support with the tensile testing machine and Michele  
671 Lonati for his help on the identification of graminoid species.

672

## 673 **References**

674

675 Abe, K., Ziemer, R.R., 1991. Effect of tree roots on a shear zone: modeling  
676 reinforced shear stress. *Canadian Journal of Forest Research* 21, 1012-1019.

677 Alpandino, 2011. Alpandino by Institute of Botany, University of Basel, Switzerland.

678 <https://www.alpandino.org>

679 Aravena, J.E., Berli, M., Ghezzehei, T.A., Tyler, S.W., 2011. Effects of root-induced  
680 compaction on rhizosphere hydraulic properties X-ray microtomography  
681 imaging and numerical simulations. *EnvSci & Tech*, 45, 425–431.

682 Bardgett, R.D., Mommer, L., De Vries, F.T., 2014. Going underground: root traits as  
683 drivers of ecosystem processes. *Trends in Ecology and Evolution*, 29, 12, 692-  
684 699.

685 Bast, A., Wilcke, W., Graf, F., Lüscher, P., Gärtner, H., 2015. A simplified and rapid  
686 technique to determine an aggregate stability coefficient in coarse-grained  
687 soils. *Catena*, 127, 170-176.

688 Bischetti, G.B., Bassanelli, C., Chiaradia, E.A., Minotta, G., Vergani, C., 2016. The  
689 effect of gap openings on soil reinforcement in two conifer stands in northern  
690 Italy. *Forest Ecology and Management*, 359, 286–299.

691 Bischetti, G.B., Chiaradia, E.A., Epis, T., Morlotti, E., 2009. Root cohesion of forest  
692 species in Italian Alps. *Plant and Soil*, 324, 71-89.

693 Bischetti, G.B., Chiaradia, E.A., Simonato, T., Speziali, B., Vitali, B., Vullo, P., Zocco,  
694 A., 2005. Root strength and root area ratio of forest species in Lombardy  
695 (Northern Italy). *Plant and Soil*, 278, 11–22

696 Bordoni, M., Meisina, C., Vercesi, A., Bischetti, G.B., Chiaradia, E.A., Vergani, C.,  
697 Chersich, S., Valentino, R., Bittelli, M., Comolli, R., Persichillo,  
698 M.G., Cislighi, A., 2016. Quantifying the contribution of grapevine roots to  
699 soil mechanical reinforcement in an area susceptible to shallow landslides.  
700 *Soil and Tillage*, 163, pp. 195-206.

701 Boundless. "Diamagnetism and Paramagnetism." *Boundless Chemistry* Boundless,  
702 08 Aug. 2016. Retrieved 03 Mar. 2017.  
703 [https://www.boundless.com/chemistry/textbooks/boundless-chemistry-](https://www.boundless.com/chemistry/textbooks/boundless-chemistry-textbook/periodic-properties-8/electron-configuration-68/diamagnetism-and-paramagnetism-320-10520/)  
704 [textbook/periodic-properties-8/electron-configuration-68/diamagnetism-and-](https://www.boundless.com/chemistry/textbooks/boundless-chemistry-textbook/periodic-properties-8/electron-configuration-68/diamagnetism-and-paramagnetism-320-10520/)  
705 [paramagnetism-320-10520/](https://www.boundless.com/chemistry/textbooks/boundless-chemistry-textbook/periodic-properties-8/electron-configuration-68/diamagnetism-and-paramagnetism-320-10520/)

706 Bradley, J.A., Singarayer, J.S., Anesio, A.M., 2014. Microbial community dynamics in  
707 the forefield of glaciers. *Peoc. R. Soc.B* 281: 20140882.

708  
709 [Broglia](#), M., Bovio, M., [Poggio](#), L., 2008. Guida alla flora della Valle d'Aosta.

710 D'Amico, M.E., Freppaz, M., Filippa, G., Zanini, E., 2014. Vegetation influence on  
711 soil formation rate in a proglacial chronosequence (Lys Glacier, NW Italian  
712 Alps). *CATENA*, 113, 122-137.

713 Gaudet, C.L., Keddy, P.A., 1988. A comparative approach to predicting competitive  
714 ability from plant traits. *Nature*, 334, 242–3

715 Ghestem, M., Sidle, R.C., Stokes, A., 2011. The influence of plant root system on  
716 subsurface flow: Implications for slope stability. *BioScience*, 61, 869-879.

717 Gonzalez-Ollauri, A., Mickovski, S.B., 2016. Using the root spread information of  
718 pioneer plants to quantify their mitigation potential against shallow landslides  
719 and erosion in temperate humid climates. *Ecological Engineering*, 95, 302-  
720 315.

721 Gonzalez-Ollauri, A., Mickovski, S.B., 2017. Plant-soil reinforcement response under  
722 different soil hydrological regimes. *Geoderma*, 285, 141-150.

723 Gregory, P.J., Hutchinson, D.J., Read, D.B., Jenneson, P.M., Gilboy, W.B., Morton,  
724 E.J., 2003. Non-invasive imaging of roots with high resolution X-Ray micro-  
725 tomography. *Plant Soil*, 255, 351–359.

726 Graf, F., Frei, M., 2013. Soil aggregate stability related to soil density, root length,  
727 and mycorrhiza using site-specific *Alnus incana* and *Melanogaster variegatus*  
728 I.. *Ecological Engineering*, 57, 314-323.

729 Grey, D.H., Sotir, R.B., 1996. Biotechnical and soil bioengineering slope stabilization.  
730 In: *A practical guide for erosion control*. Wiley, John & Sons, New York, pp. 1-  
731 105.

732 Han, L., Dutilleul, P., Prasher, S.O., Beaulieu, C., Smith, D.L., 2008. Assessment of  
733 common scab-induced pathogen effects on potato underground organs via  
734 computed tomography scanning. *Phytopathology*, 98, 1118–1125.

735 Holzmann, H., Haselwandter, K., 1988. Contribution of nitrogen fixation to nitrogen  
736 nutrition in an alpine sedge community (*Caricetum curvulae*). *Oecologia*, 76,  
737 298-302. doi: 10.1007/BF00379967

738 Hu, X., Brierley, G., Zhu, H., Li, G., Fu, J., Mao, X., Yu, Q., Qiao, N., 2013. An  
739 exploratory analysis of vegetation strategies to reduce shallow landslide activity  
740 on loess hillslopes, Northeast Qinghai-Tibet Plateau, China. *J. Mt. Sci.*, 10,  
741 668–686.

742 Hu, X., Li, Z.C., Li, X.Y., Liu, L.Y., 2016. Quantification of soil macropores under  
743 alpine vegetation using computed tomography in the Qinghai Lake Watershed,  
744 NE Qinghai–Tibet Plateau. *Geoderma*, 264,244-251.

745 Hudek, C., Stanchi, S., D’Amico, M., Freppaz, M., (submitted) Quantifying the  
746 contribution of the root system of alpine vegetation in the soil aggregate stability  
747 of moraine.

748 IBM Corp. Released 2013. IBM SPSS Statistics for Windows, Version 22.0. Armonk,  
749 NY: IBM Corp.

750 Jenneson, P.M., Gilboy, W.B., Morton, E.J., Luggar, R.D., Gregory, P.J., Hutchinson,  
751 D., 1999. Optimisation of X-ray microtomography for the in situ study of the  
752 development of plant roots. 1999 IEEE Nuclear Science Symposium  
753 Conference Record, 1–3, 429–432.

754 Jonasson, S., and Callaghan, T.V., 1992. Root Mechanical Properties Related to  
755 Disturbed and Stressed Habitats in the Arctic. *The New Phytologist* 122, 179-  
756 186.

757 Jones, G.A. and Henry, G.H.R., 2003. Primary plant succession on recently  
758 deglaciaded terrain in the Canadian High Arctic. *Journal of Biogeography*, 30,  
759 277–296. doi:10.1046/j.1365-2699.2003.00818.x

760 Kaestner, A., Schneebeli, M., Graf, F., 2006. Visualizing three-dimensional root  
761 networks using computed tomography. *Geoderma*, 136, 459–469.

762 Khan, M.A., Gemenet, D.C., Villordon, A., 2016. Root System Architecture and  
763 Abiotic Stress Tolerance: Current Knowledge in Root and Tuber Crops. *Front.*  
764 *Plant Sci.*, 7, Article 1584.

765 Koebernick, N., Weller, U., Huber, K., Schlüter, S., Vogel, H.J., Jahn, R.,  
766 Vereecken,H., Vetterlein, D., 2014. *In situ* visualization and quantification of



767 three-dimensional root system architecture and growth using x-ray computed  
768 tomography. *Vadose Zone*, 13, 1-10.

769 Körner, C., 2003. *Alpine plant life Functional plant ecology of high mountain*  
770 *ecosystems*. Springer-Verlag Berlin.

771 Kuka, K., Illerhaus, B., C.A., Fox, Joschko, M., 2013. X-ray Computed  
772 Microtomography for the Study of the Soil–Root Relationship in Grassland  
773 Soils. *Vadose Zone Journal*, 12, 1-10.

774 Lazzaro, A., Franchini, A.G., Brankatschk, R., Zeyer, J., 2010. Pioneer communities  
775 in the forefields of retreating glaciers: how microbes adapt to a challenging  
776 environment. In: *Current Research, Technology and Education Topics in*  
777 *Applied Microbiology and Microbial Biotechnology* (Edi.Mendes-Villas, A.)  
778 *Formatex*, Badajoz, Spain.

779 Lichtenegger, E., 1996. Root distribution in some alpine plants. *Acta Phytogeogr.*  
780 *Suec.*, 81, 76-82.

781 Lichtenegger, E., and Kutschera-Nitter, L., 1991. Spatial root types. In Edited by  
782 McMichael, B.L., and Persson, H. *Development in agricultural and managed*  
783 *forests ecology 24. Plant roots and their environment. Proceedings of an ISRR*  
784 *symposium Elsevier Science Publisher B.V. Amsterdam, Netherlands.*

785 Lobet, G., Pound, M.P., Diener, J., Pradal, C., Drayer, X., Godin, C., Javaux, M.,  
786 Leitner, D., Maunier, F., Nancy, P., Pridmore, T.P., Schnepf, A., 2015. Root  
787 system markup language: toward a unified root architecture description  
788 language. *Plant Physiology*, 167, 617-627.

789 Lontoc-Roy, M., Dutilleul, P., Prasher, S.O., Han, L., Brouillet, T., Smith, D.L., 2006.  
790 *Advances in the acquisition and analysis of CT scan data to isolate a crop root*

791 system from the soil medium and quantify root system complexity in 3-Dspace.  
792 Geoderma, 137, 231–241.

793 Mairhofer, S., Sturrock, C., Wells, D.M., Bennett, M.J., Mooney, S.J., Pridmore, T.P.,  
794 2015. On the evaluation of methods for the recovery of plant root systems  
795 from X-ray computed tomography images. Functional Plant Biology, 42, 460–  
796 470.

797 Mairhofer, S., Zappala, S., Tracy, S.R., Sturrock, C., Bennett, M., Mooney, S.J.,  
798 Pridmore, T., 2012. RooTrak: Automated Recovery of Three-Dimensional  
799 Plant Root Architecture in Soil from X-Ray Microcomputed Tomography  
800 Images Using Visual Tracking. Plant Physiology, 158, 561–569.

801 Massaccesi, L., Benucci, G.M.N., Gigliotti, G., Cocco, S., Corti, G., Agnelli, A., 2015.  
802 Rhizosphere effect of three plant species of environment under periglacial  
803 conditions (Majella massif, central Italy). Soil Biology and Biochemistry, 89,184-  
804 195.

805 Matthews, J.A., 1999. Disturbance regimes and ecosystem response on recently-  
806 deglaciated terrain. In Ecosystems of Disturbed Ground, Walker LR (ed.).  
807 Elsevier: Amsterdam; 17–37.

808 Mercalli, L., 2003. Atlante climatic della Valle d’Aosta. Societa Meteorologica Italia,  
809 Torino 405.

810 Mooney, S.J., Morris, C., Berry, P.M., 2006. Visualization and quantification of the  
811 effects of cereal root lodging on three-dimensional soil macrostructure using X-  
812 ray Computed Tomography. Soil Sci, 171, 706–718.

813 Mooney, S.J., Pridmore, T.P., Helliwell, J., Bennett, M.J., 2012. Developing X-ray  
814 Computed Tomography to non-invasively image 3-D root systems architecture  
815 in soil. Plant Soil, 352, 1-22.

816 Nagel, K.A., Putz, A., Gilmer, F., Heinz, K., Fischbach, A., Pfeifer, J., Faget, M.,  
817 Blossfeld, S., Ernst, M., Dimaki, C., Kastenholz, B., Kleinert, A.K., Galinski, A.,  
818 Scharr, H., Fiorani, F., Schurr, U., 2012. GROWSCREEN-Rhizo is a novel  
819 phenotyping robot enabling simultaneous measurements of root and shoot  
820 growth for plants grown in soil-filled rhizotrons. *Functional Plant Biology*, 39,  
821 891-904. <http://dx.doi.org/10.1071/FP12023>

822 Nagelmüller, S., Hiltbrunner, E., Körner, C., 2016. Critically low soil temperatures for  
823 root growth and root morphology in three alpine plant species. *Alp Botany*  
824 126, 11–21.

825 Norris, J.E., Stokes, A., Mickovski, S.B., Cammeraat, E., Van Beek, R., Nicoll, B.C.,  
826 Achim, A., 2008. Slope stability and erosion control: ecotechnological  
827 solutions. Springer, Dordrecht.

828 Ola, A., Dodd, I.C., Quinton, J.N., 2015. Can we manipulate root system architecture  
829 to control soil erosion? *SOIL*, 1, 603-612.

830 Onipchenko, V.G., Kipkeev, A.M., Makarov, M.I., Kozhevnikova, A.D., Ivanov, V.B.,  
831 Soudzilovskaia, N.A., Tekeev, D.K., Salpagarova, F.S., Werger, M.J.A.,  
832 Cornelissen, J.H.C., 2014. Digging deep to open the white black box of snow  
833 root phenology. *Ecol Res*, 29, 529–534.

834 Paez-Garcia, A., Motes, C.M., Scheible, W.-R., Chen, R., Blancaflor, E.B., Monteros,  
835 M.J., 2015. Root Traits and Phenotyping Strategies for Plant  
836 Improvement. *Plants*, 4, 334–355.

837 Paya, A.M., Silverberg, J., Padgett, J., Bauerle, T.L., 2015. X-ray computed  
838 tomography uncovers root-root interactions: quantifying spatial relationships  
839 between interacting root systems in three dimensions. *Frontiers in Plant*  
840 *Science*, 6, 274.

841 Pérez-Harguindeguy, N., Díaz, S., Garnier, E., Lavorel, S., Poorter, H.,  
842 Jaureguiberry, P., Bret-Harte, M.S., Cornwell, W.K., Craine, J.M., Gurvich,  
843 D.E., Urcelay, C., Veneklaas, E.J., Reich, P.B., Poorter, L., Wright, I.J., Ray,  
844 P., Enrico, L., Pausas, J.G., de Vos, A.C., Buchmann, N., Funes, G., Quétier,  
845 F., Hodgson, J.G., Thompson, K., Morgan, H.D., ter Steege, H., van der  
846 Heijden, M.G.A., Sack, L., Blonder, B., Poschlod, P., Vaieretti, M.V., Conti, G.,  
847 Staver, A.C., Aquino S., Cornelissen, J.H.C., 2013. New handbook for  
848 standardised measurement of plant functional traits worldwide. *Australian*  
849 *Journal of Botany*, 61, 167–234.

850 Pierret, J.S., Prasher, S.O., Kantzas, A., Langford, C., 1999. Three-dimensional  
851 quantification of macropore networks in undisturbed soil cores. *Soil Sci. Soc.*  
852 *Am. J*, 63, 1530–1543.

853 Pierret, A., Moran, C., Doussan, C., 2005. Conventional detection methodology is  
854 limiting our ability to understand the roles and functions of fine roots. *New*  
855 *Phytol*, 166, 967–980.

856 Pignatti, S., 2003. *Flora D'Italia*. Vol.3. Edagricole S.r.l., Bologna.

857 Pfeifer, J., Kirchgessner, N., Colombi, T., Walter, A., 2015. Rapid phenotyping of  
858 crop root systems in undisturbed field soil using X-ray computed tomography.  
859 *Plant Methods*, 11, 41.

860 Pfeifer, J., Faget, M., Walter, A., Blossfeld, S., Fiorani, F., Schurr, U., Nagel, K.A.,  
861 2014. Spring barley shows dynamic compensatory root and shoot growth  
862 responses when exposed to localised soil compaction and fertilisation.  
863 *Functional Plant Biology*, 41, 581-597.

864 Pohl, M., Alig, D., Körner, C., Rixen, C., 2009. Higher plant diversity enhances soil  
865 stability in disturbed alpine ecosystems. *Plant Soil*, 324, 91–102.

866 Pohl, M., Stroude, R., Buttler, A., Rixen, C., 2011. Functional traits and root  
867 morphology of alpine plants. *Annals of Botany*, 108, 537–545,  
868 doi:10.1093/aob/mcr169

869 Poorter, H., Niklas, K.J., Reich, P.B., Oleksyn, J., Poot, P., Mommer, L., 2012.  
870 Biomass allocation to leaves, stems and roots: meta-analyses of interspecific  
871 variation and environmental control. *New Phytologist*. 193, 30-50.

872 Reubens, B., Poesen, J., Danjon, F., Geudens, G., Muys, B., 2007. The role of fine  
873 and coarse roots in shallow slope stability and soil erosion control with a focus  
874 on root system architecture: a review. *Trees*, 21, 385–402.

875 Robbins, J.A., Matthews, J.A., 2009. Pioneer vegetation on glacier forefields in  
876 southern Norway: emerging communities? *Journal of Vegetation Science*, 20,  
877 889-902.

878 Sati, S.P., Sundriyal, Y.P., 2007. Role of some species in slope instability.  
879 *Himalayan Geol.*, 28, 75-78.

880 Smith, S.E., Read, D.J., 2008. *Mycorrhizal Symbiosis*. Academic Press, Cambridge.

881 Soil Survey Staff, 2010. *Keys to soil Taxonomy*. United States Department of  
882 Agriculture, Eleventh edition. Natural Resources Conservation Services.

883 Stokes, A., Atger, C., Bengough, A.G., Fourcaud, T., Sidle, R.C., 2009. Desirable  
884 plant root traits for protecting natural and engineered slopes against landslides.  
885 *Plant Soil*, 324, 1-30.

886 Stöcklin, J., Bäumler, E., 1996. Seed rain, seedling establishment and clonal growth  
887 strategies on a glacier foreland. *Journal of Vegetation Science.*, 9, 45-56.

888 Stöcklin, J., Kuss, P., Pluess, A.R., 2009. Genetic diversity, phenotypic variation and  
889 local adaptation in the alpine landscape: case studies with alpine plant  
890 species. *Bot.Helv.*119, 125-133.

- 891 Tasser, E., Tappeiner, U., 2005. New model to predict rooting in diverse plant  
892 community compositions. *Ecological Modelling*, 185, 195-211.
- 893 Tisdall, J.M., 1991. Fungal hyphae and structural stability of soil. *Australian Journal*  
894 *of Soil Research*, 29, 729-743.
- 895 Tollner, E.W., Rasmseur, E.L., Murphy, C., 1994. Techniques and approaches for  
896 documenting plant root development with X-ray computed tomography. In  
897 *Tomography of soil water-root processes*. Edited by Anderson, S.H., and  
898 Hopmans, J.W., SSSA Special Publication, 36, Madison, Wis. 115–133.
- 899 Tracy, S.R., Black, C.R., Roberts, J.A., Sturrock, C., Mairhofer, S., Craigon, J.,  
900 Mooney, S.J., 2012. Quantifying the impact of soil compaction on root system  
901 architecture in tomato (*Solanum lycopersicum*) by X-ray micro-computed  
902 tomography. *Ann. Bot.*, 110, 511-519.
- 903 Wantanabe, K., Mandang, T., Tojo, S., Ai, F., Huang, B.K., 1992. Non-destructive  
904 root-zone analysis with X-ray CT scanner. Paper 923018. American Society of  
905 Agricultural Engineers. St Joseph, MI, USA
- 906 Yang, Y., Chen, L., Li, N., & Zhang, Q., 2016. Effect of Root Moisture Content and Diameter  
907 on Root Tensile Properties. *PLoS ONE*, 11, e0151791.
- 908 Zoller, H., and Lenzin, H., 2006. Composed cushions and coexistence with  
909 neighbouring species promoting the persistence of *Eritrichium nanum* in high  
910 alpine vegetation. *Bot. Helv.*, 116, 31–40.

911

912

913

914

915

916 **Table and Figure Captions**

917 **Table 1**

918

919 **Table 2** Scanning parameters for X-ray CT.

920

921 **Table 3** Values of root traits analyzed with RooTrak (volume, area, maximum vertical  
922 and horizontal length of the root system, convex hull), ImageJ (maximum vertical and  
923 horizontal length of the root system) and WinRHIZO (total root length and average  
924 root diameter) of the X-ray CT scanned samples.

925

926 **Table 4** Plant height (mm), rooting depth (mm) measured with ImageJ, total root  
927 length (m), mean root diameter (mm) and root length density ( $\text{cm cm}^{-3}$ ) of the 10  
928 studied alpine species measured with WinRHIZO.

929

930 **Table 5** Root length distribution (%) of the 10 pioneer alpine plants in relation to  
931 different diameter classes (mm).

932

933 **Table 6** Life forms, the number of samples (n) tested, the range of root diameters  
934 (mm), root tensile strength (MPa) values, scale factor ( $\alpha$ ) rate of strength decrease  
935 ( $\beta$ ) and the goodness of fit ( $R^2$ ) of the 10 studied alpine species.

936

937 **Table 7** ANOVA table with multiple comparisons of root tensile strength (MPa)  
938 between the studied plant species.

939

940 **Figure 1 a - j** Root architecture of the 10 studied pioneer alpine species detected by  
941 X-ray CT scanning. a., *E. fleischeri*; b., *F. halleri*; c., *L. alpine*; d., *L. spicata*; e., *M.*  
942 *recurva*; f., *P. laxa*; g., *S. helvetica*; h., *S. exscapa*; i., *T. pallescens*; j., *T.*  
943 *distichophyllum*; Scale bars: a., 35 mm, b., 25 mm, c., 40 mm, d., 15 mm, e., 10  
944 mm, f., 15 mm, g., 15 mm, h., 30 mm, i., 45 mm, j., 20 mm.

945

946 **Figure 2** a., Image of the core root system b., the core root system in relation to the  
947 soil matrix and c., the washed entire root system of *Trifolium pallescens*. Scale bar  
948 a., 45 mm b., 40 mm and c., the ruler uses cm.

949

950 **Figure 3** a., Linear correlation between RooTrak and ImageJ data on the maximum  
951 vertical and b., horizontal root length for the 10 studied alpine species.

952

953 **Figure 4**

954

955 **Figure 5** Examples of the grayscale CT images of the soil matrices a., glacial till with  
956 *T. distichophyllum* b., and c., fluvio-glacial and lake depositions.

957

958 **Figure 6** Plant height (cm) and rooting depth (cm) of the 10 studied alpine plant  
959 species.

960

961 **Figure 7** The relationship between root tensile strength (MPa) and root diameter  
962 (mm) for the 10 studied alpine species.

963

964



965 **Table 1**

Species	Common name	Life form	Succession	Family
<i>Epilobium fleischeri</i> Hochst.	Alpine willowherb	Forb	Early	Omagraceae
<i>Trisetum distichophyllum</i> (Vill.) P.Beauve.	Tufted hairgrass	Graminoid	Early	Poaceae
<i>Trifolium pallescens</i> Schreb.	Pale clover	Forb	Early	Fabaceae
<i>Luzula spicata</i> (L.) DC.	Spiked woodrush	Graminoid	Mid	Juncaceae
<i>Silene exscapa</i> All.	Moss campion	Forb	Mid	Caryophyllaceae
<i>Minuartia recurva</i> (All.) Schinz and Thell.	Recurved sandwort	Forb	Late	Caryophyllaceae
<i>Festuca halleri</i> All.	Haller's Fescue	Graminoid	Late	Poaceae
<i>Poa laxa</i> Haenke	Banff Bluegrass	Graminoid	Ubiquitous	Poaceae
<i>Salix helvetica</i> Vill.	Swiss willow	Dwarf shrub	Ubiquitous	Salicaceae
<i>Leucanthemopsis alpina</i> (L.) Heyw.	Alpine Moon Daisy	Forb	Ubiquitous	Asteraceae

966

967

968

969 **Table 2** Scanning parameters for X-ray CT.

Voltage (kV)	Current (µA)	Number of projections	Exposure time (ms)	Resolution (µm)	Signal averaging	Total scanning time
180	160	2160	250	54	4/1	2h17min

970

971 **Table 3** Values of root traits analyzed with RooTrak (volume, area, maximum vertical  
 972 and horizontal length of the root system, convex hull), ImageJ (maximum vertical and  
 973 horizontal length of the root system) and WinRHIZO (total root length and average  
 974 root diameter) of the X-ray CT scanned samples.

Plant species	Root type	RooTrak				ImageJ		
		Volume (mm <sup>3</sup> ) (total mass of the root system)	Area (mm <sup>2</sup> ) (root area in direct contact with the soil)	Depth (mm) (root system's maximum vertical distance)	Width (mm) (root system's maximum horizontal distance)	Convex hull (mm <sup>2</sup> ) (region of soil explored by the root system)	Vertical length (mm)	Horizontal length (mm)
<i>T. distichophyllum</i>	Cylindrical	353	3399	63	68	65774	75	7
<i>E. fleischeri</i>	Pole	967	3711	105	65	90931	115	7
<i>T. pallescens</i>	Cone↑	1530	7752	132	72	505364	225	7
<i>S. exscapa</i>	Cone↑	385	2383	102	70	357053	173	6
<i>L. spicata</i>	Cone↓	306	2106	39	71	27046	137	7
<i>F. halleri</i>	Cone↓	828	5866	67	71	60318	107	5
<i>M. recurva</i>	Discoid	144	1677	44	68	60237	164	5
<i>P. laxa</i>	Cone↓	150	1547	33	72	45612	119	3
<i>L. alpina</i>	Umbrella	542	4666	126	72	224012	141	6
<i>S. helvetica</i>	Discoid	435	1146	35	73	24117	49	3

975

976 **Table 4** Plant height (mm), rooting depth (mm) measured with ImageJ, total root  
 977 length (m), mean root diameter (mm) and root length density (cm cm<sup>-3</sup>) of the 10  
 978 studied alpine species measured with WinRHIZO.

Plant species	Plant height (mm)	Rooting depth (mm)	Total root length (m)	Mean root diameter (mm)	Root length density (cm cm <sup>-3</sup> )
<i>T. distichophyllum</i>	50	133	336.9	0.21	85
<i>E. fleischeri</i>	65	197	75.3	0.23	9
<i>T. pallescens</i>	47	133	197.6	0.47	33
<i>S. exscapa</i>	20	153	106.2	0.33	49
<i>L. spicata</i>	30	117	202.1	0.22	81
<i>F. halleri</i>	32	101	297.8	0.35	59
<i>M. recurva</i>	15	118	135.9	0.32	29
<i>P. laxa</i>	51	119	210.1	0.28	47
<i>L. alpina</i>	20	127	368.5	0.26	53
<i>S. helvetica</i>	25	90	342.3	0.27	68

979

980 **Table 5** Root length distribution (%) of the 10 pioneer alpine plants in relation to  
 981 different diameter classes (mm).

	0<L<0.1	0.1<L<0.2	0.2<L<0.3	0.3<L<0.4	0.4<L<0.5	0.5<L<0.75	0.75<L<1
<i>T. distichophyllum</i>	33	41	15	5	2	1	
<i>T. pallescens</i>	49	19	10	5	4	6	
<i>S. exscapa</i>	42	30	12	5	3	4	
<i>L. spicata</i>	57	27	9	3	1	1	
<i>F. halleri</i>	37	22	15	8	5	7	
<i>M. recurva</i>	36	30	13	6	3	5	
<i>P. laxa</i>	49	19	12	6	4	5	
<i>L. alpina</i>	36	29	14	7	5	5	
<i>S. helvetica</i>	9	25	37	6	4	4	

982

983 **Table 6** Life forms, the number of samples (n) tested, the range of root diameters  
 984 (mm), root tensile strength (MPa) values, scale factor (α) rate of strength decrease  
 985 (β) and the goodness of fit (R<sup>2</sup>) of the 10 studied alpine species.

Species	Life form	n	d range (mm)	Mean Tr (MPa)	α	β	R <sup>2</sup>	p
<i>T. distichophyllum</i>	Graminoid	30	0.05-1.15	86	23.26	0.62	0.56	<0.001
<i>E. fleischeri</i>	Forb	32	0.04-1.56	58	3.61	1.15	0.67	<0.001
<i>T. pallescens</i>	Forb	32	0.05-1.66	44	10.55	0.88	0.65	<0.001
<i>S. exscapa</i>	Forb	30	0.03-1.14	54	11.85	0.84	0.65	<0.001
<i>L. spicata</i>	Graminoid	30	0.03-0.37	138	9.54	1.01	0.71	<0.001
<i>F. halleri</i>	Graminoid	30	0.05-0.46	94	17.92	0.75	0.70	<0.001
<i>M. recurva</i>	Forb	30	0.03-0.35	60	6.24	1.11	0.78	<0.001

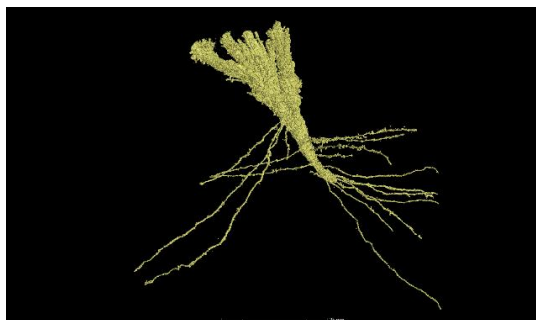
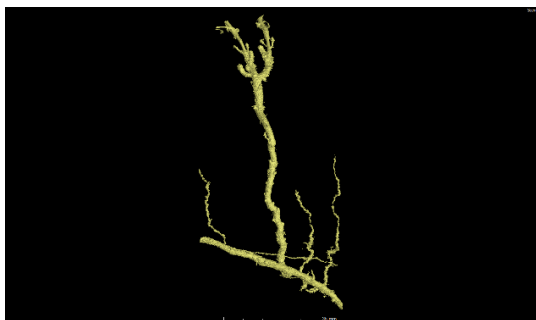
<i>P. laxa</i>	Graminoid	30	0.03-0.56	113	21.65	0.75	0.82	<0.001
<i>L. alpina</i>	Forb	32	0.05-0.59	29	8.67	0.75	0.71	<0.001
<i>S. helvetica</i>	Dwarf shrub	30	0.03-0.78	110	11.34	0.94	0.78	<0.001

986

987 **Table 7** ANOVA table with multiple comparisons of root tensile strength (MPa)  
 988 between the studied plant species.

989

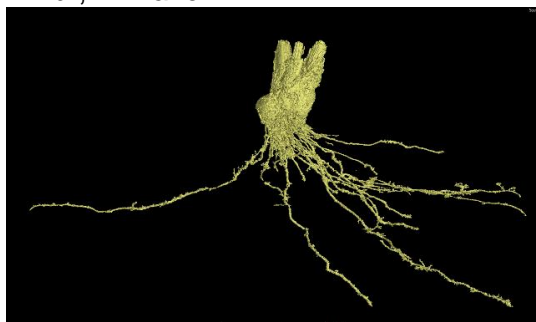
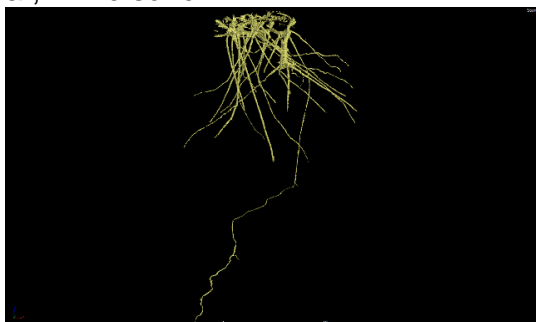
990 **Figure1 a - j** Root architecture of the 10 studied pioneer alpine species detected by  
 991 X-ray CT scanning. a., *E. fleischeri*; b., *F. halleri*; c., *L. alpina*; d., *L. spicata*; e., *M.*  
 992 *recurva*; f., *P. laxa*; g., *S. helvetica*; h., *S. exscapa*; i., *T. pallescens*; j., *T.*  
 993 *distichophyllum*; Scale bars: a., 35 mm, b., 25 mm, c., 40 mm, d., 15 mm, e., 10  
 994 mm, f., 15 mm, g., 15 mm, h., 30 mm, i., 45 mm, j., 20 mm.



995  
 996

a., *E. fleischeri*

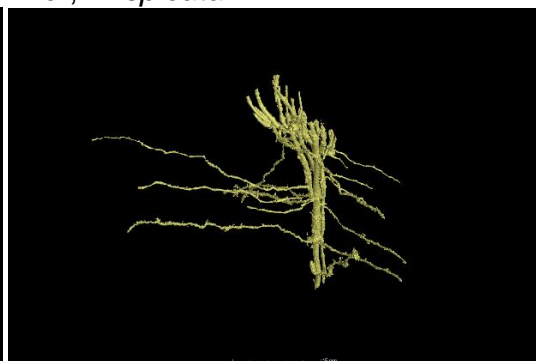
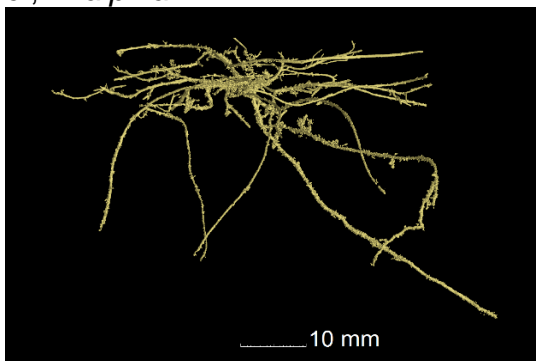
b., *F. halleri*



997  
 998

c., *L. alpina*

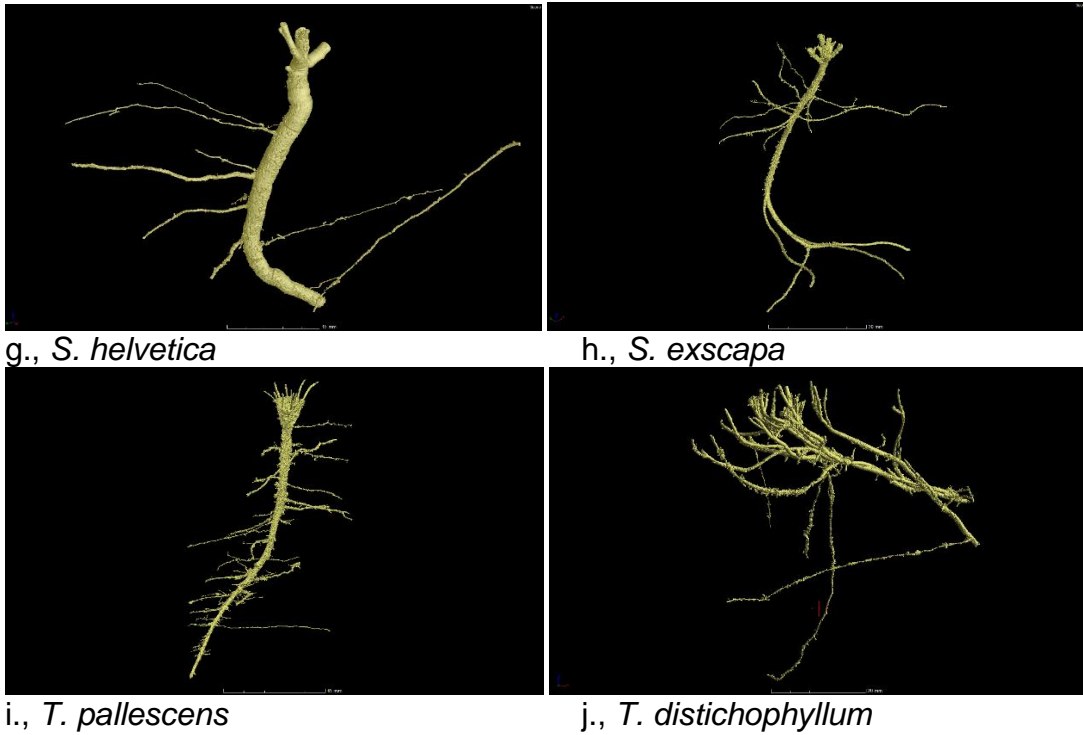
d., *L. spicata*



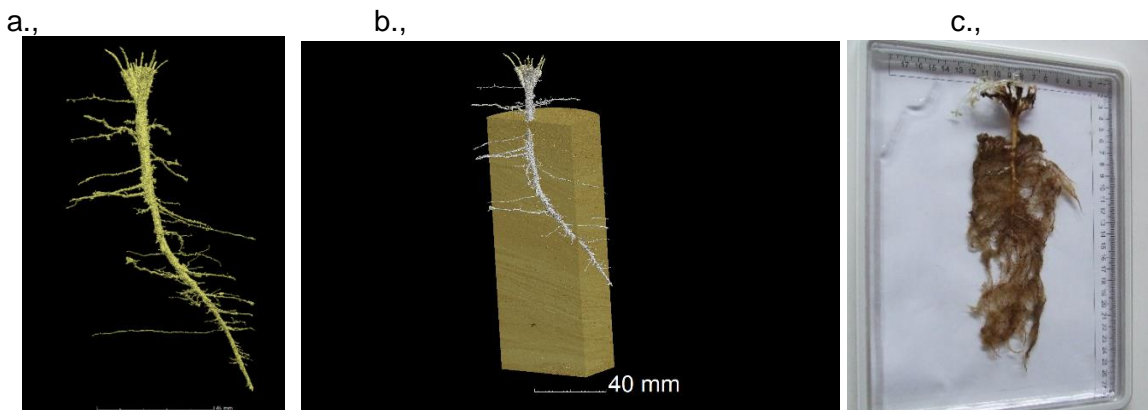
999  
 1000

e., *M. recurva*

f., *P. laxa*

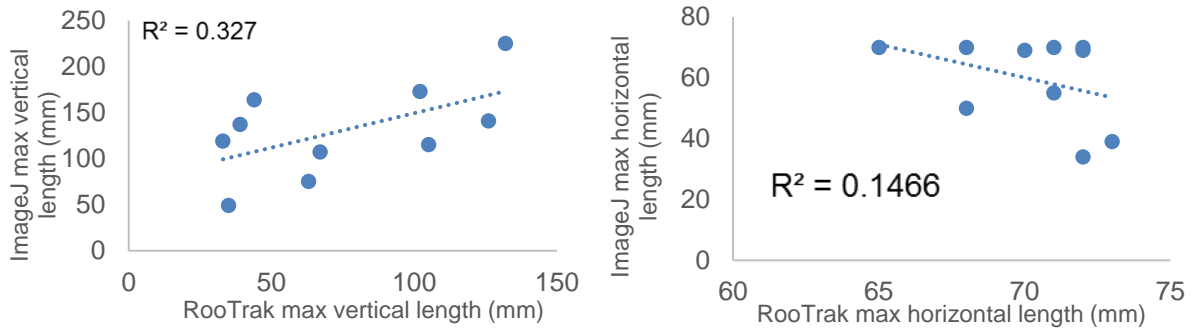


1005 **Figure 2** a., Image of the cored root system b., the core root system in relation to the  
 1006 soil matrix and c., the washed entire root system of *Trifolium pallescens*. Scale bar  
 1007 a., 45 mm b., 40 mm and c., the ruler uses cm.



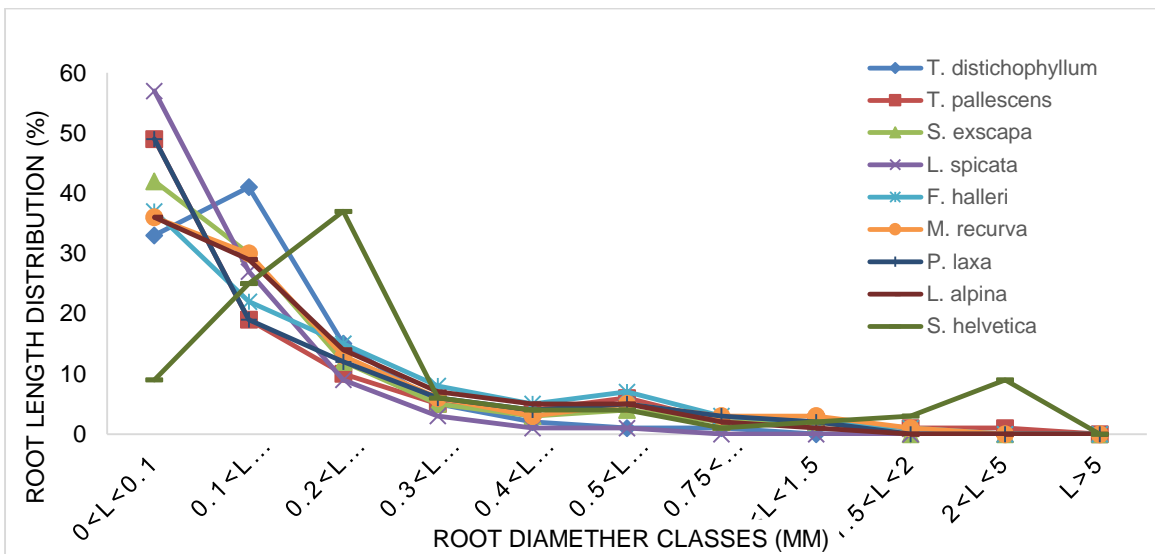
1013 **Figure 3** a., Linear correlation between RooTrak and ImageJ data on the maximum  
 1014 vertical and b., horizontal root length for the 10 studied alpine species.

1015 a., b.,



1016

1017 **Figure 4**



1018

1019

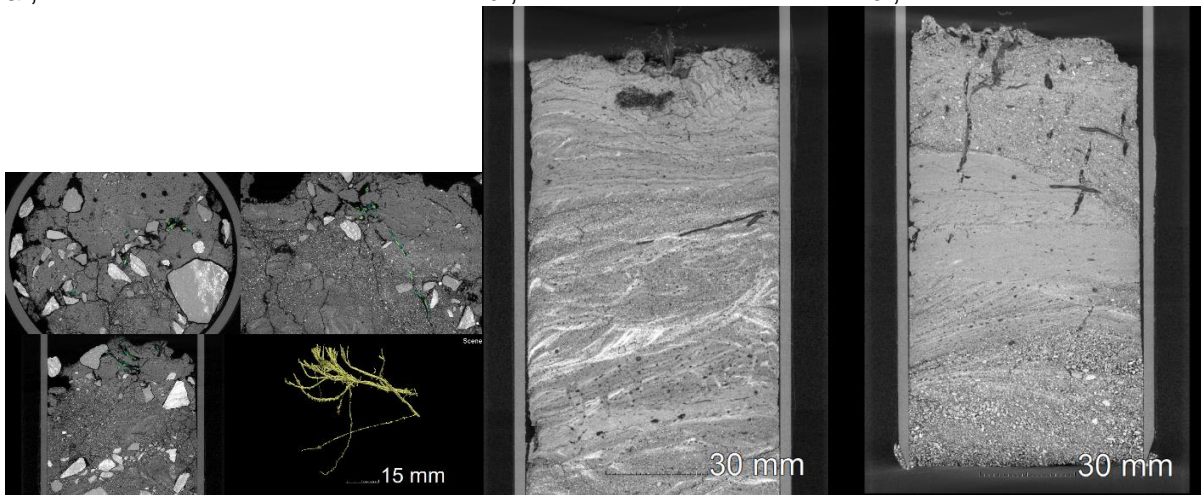
1020 **Figure 5** Examples of the grayscale CT images of the soil matrices a., glacial till with  
 1021 *T. distichophyllum* b., and c., fluvio-glacial and lake depositions.

1022

1023 a.,

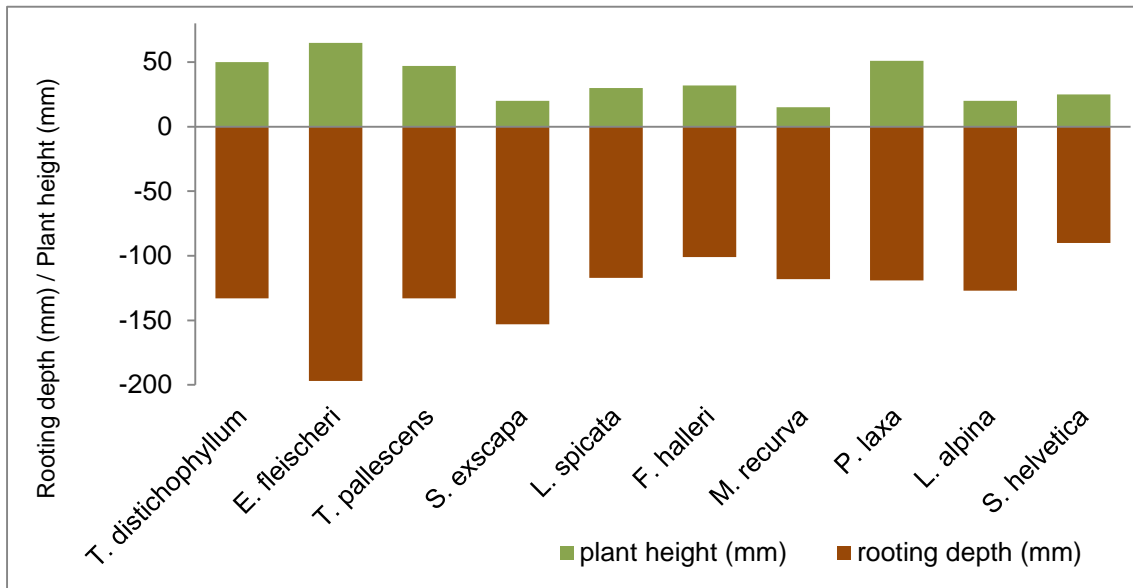
b.,

c.,



1024

1025



1026 **Figure 6** Plant height (cm) and rooting depth (cm) of the 10 studied alpine plant species.

1027

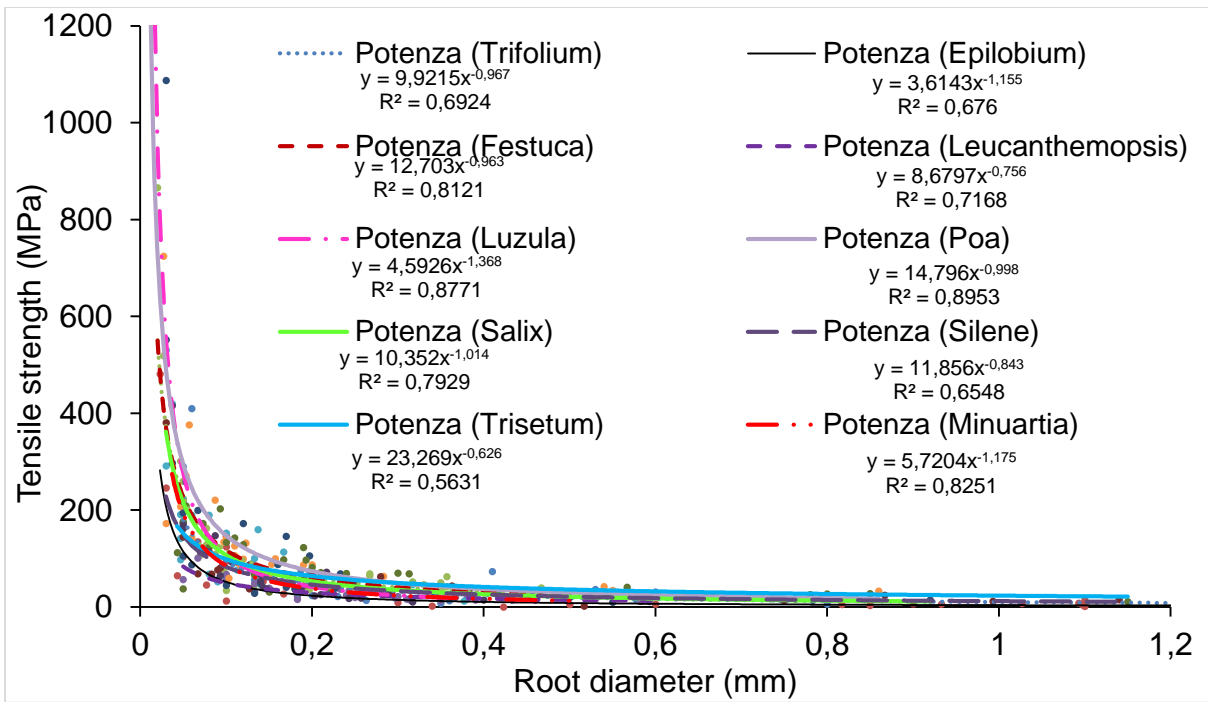
1028

1029

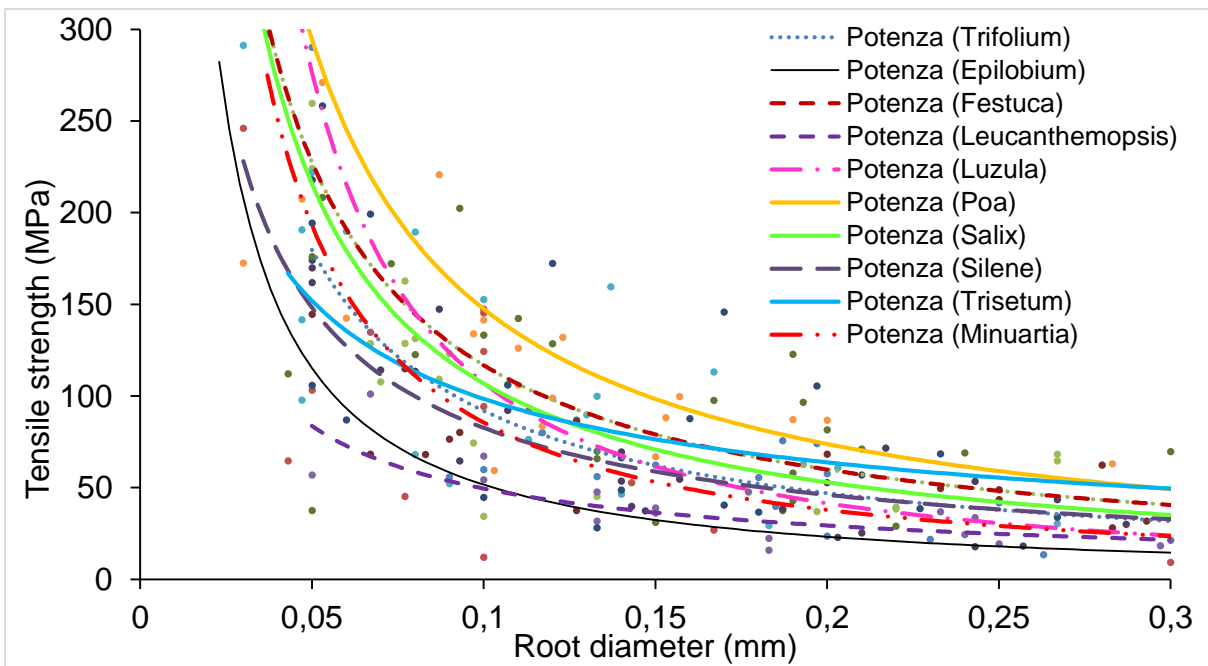
1030

1031 **Figure 7** The relationship between root tensile strength (MPa) and root diameter

1032 (mm) for the 10 studied alpine species



1033



1034